npj | breast cancer

Article

Published in partnership with the Breast Cancer Research Foundation

Article in Press

https://doi.org/10.1038/s41523-026-01048-2

Estrogen modulates NK and CD8 + T cell response via the PD-1 PD-L1 axis impairing antitumour effects of zoledronic acid

Check for updates

Christopher George[1,6], Jiabao Zhou[1,6], Russell Hughes[1,6], Victor Canuas-Landero[1], Diane V. Lefley[1], Fiona Thistletwaite[2,3], Caroline Wilson[1,2,4], Ingunn Holen[1], Janet E. Brown[1], Mark Dunning[1], Sarah Danson[1,4], Matthew Winter[1,4], Lewis Quayle[5], Munitta Muthana[1] & Penelope D. Ottewell[1] ✉

Clinical trials in breast cancer have demonstrated reduced recurrence in bone and soft tissue in postmenopausal women following either neoadjuvant or adjuvant treatment with Zoledronic acid (Zol). In contrast however, the same treatment resulted in an increased risk of extra-skeletal recurrence in premenopausal women. The reason for these stark differences has remained unclear, until now, preventing thousands of young breast cancer patients from being able to benefit from the life prolonging effects of Zol. Here we demonstrate that Zol induces an anti-tumor response by increasing infiltration of CD8 + T, dendritic and NK cells into soft tissue metastases, but only when estrogen concentrations are low. Anti-tumor response to Zol appears to be CD8 + T and NK cell-dependent in soft tissue, but only NK cell-dependent in bone. Conversely, elevated levels of estrogen are associated with reduced systemic and tumor infiltrating CD8+ and CD4 + T cells, increased PD-1 expression on T and NK cells, and PD-L1 on tumor cells. We propose that premenopausal concentrations of estradiol antagonize Zol-induced anti-tumor immunity, which relies on CD8 + T-cells and NK cells—an effect that is reversed by PD-1/PD-L1 blockade.

Addition of Zoledronic acid (Zol) to neoadjuvant or adjuvant standard-of-care treatment provides life prolonging, anti-metastatic, benefits for post-menopausal breast cancer patients. The same treatment does not benefit premenopausal patients[1]. This study investigates the mechanisms responsible for these differential antitumor effects with the aim of establishing methods for overcoming the absence of Zol-induced anti-metastatic effects under premenopausal conditions.

Breast cancer is the second most common malignancy globally, resulting in ~670,000 annual deaths among women[2]. Approximately 70% of breast cancer patients with advanced breast cancer will develop skeletal metastases during their disease course, which significantly reduces their life expectancy. Currently, there are no curative treatments for metastatic breast cancer[3]. However, third-generation, nitrogen-containing bisphosphonates such as Zoledronic acid (Zol) are given to breast cancer patients with bone metastasis to inhibit tumor-induced osteolytic bone resorption[4]. These anti-resorptive drugs rapidly bind to the mineral component of bone tissue, inducing apoptosis in bone-lining osteoclasts through inhibition of the mevalonate pathway[5,6]. In addition, Zol displays direct anti-tumor activity in pre-clinical models of bone and soft tissue cancers, which is further enhanced when given in combination with chemotherapy[7–11]. Large-scale clinical trials have confirmed that bisphosphonates such as Zol have significant anti-metastatic potential when given in combination with standard-of-care adjuvant therapies in breast cancer patients. The ABCSG-12 breast cancer trial reported a 29% reduction in disease recurrence in women with early breast cancer receiving Zol in combination with endocrine therapy, compared with endocrine therapy alone. This study included 1083 pre-menopausal women rendered chemically postmenopausal with ovarian suppression who received endocrine therapy (tamoxifen or anastrozole).

[1]Division of Clinical Medicine, School of Medicine and Population Health, University of Sheffield, Sheffield, UK. [2]Experimental Cancer Medicine Team, The Christie NHS Foundation Trust, Manchester, UK. [3]Division of Cancer Sciences, The University of Manchester, Manchester, UK. [4]Weston Park Hospital, Sheffield Teaching Hospitals NHS Foundation Trust, Sheffield, UK. [5]School of computing and Digital Technologies, Sheffield Hallam University, Sheffield, UK. [6]These authors contributed equally: Christopher George, Jiabao Zhou, Russell Hughes. ✉e-mail: p.d.ottewell@sheffield.ac.uk

Interestingly, Zol significantly increased overall survival in women >40 years of age ($p = 0.042$)[12]. The AZURE trial, which included 3360 patients diagnosed with early-stage II-III breast cancer, demonstrated that Zol significantly reduced the risk of metastatic disease both in bone and soft tissue when given alongside standard-of-care adjuvant therapy, in women >5 years postmenopause at the time of enrollment. Conversely, Zol significantly *increased* the risk of disease recurrence outside of bone in women <40 years of age[1]. In both studies, Zol reduced bone metastasis independent of the menopausal status of the patient. The difference in survival outcomes in pre- and postmenopausal patients receiving adjuvant Zol is attributed to reduced recurrence outside of bone in postmenopausal women, but the precise mechanisms behind this differential effect remain to be determined. Similar findings were reported in subsequent trials of neo- and adjuvant bisphosphonates (including ZO-FAST[13], NSABP-B34[14], and GAIN[15]). Taken together, clinical trial data suggest that high levels of reproductive hormones in younger women may inhibit the anti-tumor effects of bisphosphonates, resulting in premature death from visceral metastatic disease.

Analysis of serum from patients enrolled in the AZURE study, alongside laboratory modeling, has clearly identified that high levels of estrogen found in premenopausal patients are associated with inhibiting the anti-tumor effects of Zol outside bone. In the AZURE cohort, women whose circulating concentrations of 17ß-estradiol (E2) were >50 pmol/ml had shorter invasive disease-free survival following addition of Zol to standard of care ($p = 0.022$), independent of the tumor hormone receptor status[1,13,16]. Inhibiting estrogen and FSH in mice, via ovariectomy and simultaneous administration of goserelin, significantly enhanced the anti-metastatic activity of Zol (both in bone and soft tissue), compared to mice treated with sham operated mice. Conversely, restoring E2 to premenopausal levels (96–172 pg/mL) in ovariectomy/goserelin-treated mice altered the response to Zol by reducing bone metastasis but increasing soft tissue metastasis[17], mimicking data obtained in the AZURE study.

In the current study, we therefore aimed to determine the mechanisms by which the effects of E2 and Zol interact to affect tumor growth both in bone and non-bone sites in immunocompetent mouse models. We have previously shown that supplementing mice with premenopausal concentrations of E2 increases tumor cell dissemination in bone and soft tissues in immune competent mice but not in athymic mice. Furthermore, under premenopausal E2, Zol elicits anti-tumor responses in immune competent mice, reducing soft tissue tumor volume, but these effects are not seen in athymic mice[17]. As athymic mice have no mature T cells and reduced innate immune response when faced with challenge, we hypothesized that differential antitumor effects of Zol, outside of bone, are caused by E2-mediated changes to antitumor immune responses.

Results

Modeling pre- and postmenopausal estrogen levels in vivo

Using the E0771 (C57BL/6 background) and the 4T1 (BALB/c background) mouse models of breast cancer, we investigated how adding pre- and postmenopausal concentrations of E2 impacted on the anti-metastatic activity of Zol in ovariectomized mice (Fig. 1). Ovariectomy in mice resulted in baseline circulating E2 concentrations of 1.01 (+/−0.37) pg/ml and 30.8 (+/−7.3) pg/ml in BALB/c and C57BL/6 mice, respectively (postmenopausal; low). Supplementing the drinking water of ovariectomized mice with E2 increased circulating E2 levels to 153.16 (+/−18.10) pg/mL and 392.13 (+/−106.51) pg/ml in BALB/c and C57BL/6 mice, respectively (premenopausal; high) (Supplementary Fig. 1). These models share key features with the metastatic profile observed in pre- and postmenopausal women treated with adjuvant Zol: In mice with low E2, administration of Zol reduced both soft tissue metastasis ($p < 0.05$ 4T1 [BALB/c]; $p < 0.01$ E0771 [C57BL/6]; Fig. 1b) and bone metastasis ($p < 0.05$ 4T1 [BALB/c]; $p < 0.01$ E0771 [C57BL/6]; Fig. 1c). In contrast, when E2 levels were high, Zol significantly increased soft tissue metastatic burden in the E0771 model (C57BL/6) by 271% (+/−164%; $P < 0.05$) (Fig. 1d), no significant change was observed in the 4T1 model (BALB/c). Furthermore, in high E2, Zol significantly inhibited bone metastasis in the 4T1 mode (BALB/c)(Fig. 1e), but not in the E0771 (C57BL/6). Collectively, these data confirm, that like in humans, Zol is only able to exert anti-tumor effects outside of bone in low E2 conditions in mice, with some strain-specific variations in response. Changes in circulating markers of bone turnover were consistent with those reported previously[17]: Zol reduced levels of serum TRAP5b, a circulating marker of osteoclast activity, regardless of E2 status (Fig. 1f). Similar results were obtained for serum P1NP, a marker of osteoblast activity (Fig. 1g), except in BALB/c mice exposed to low E2 conditions.

Zol reshapes the splenic immune landscape in the presence of E2

E2 and Zol have established immunomodulatory effects on a variety of cell types[18–20], however, the majority of these effects have not been investigated in the context of cancer (reviewed in ref. 21). We carried out a comprehensive study to establish how Zol affects the systemic immune landscape, as well as in specific tissue environments (soft tissue and bone), and how these immune cell effects were further altered under the influence of E2. Zol had very little effect on the splenic frequency of innate immune cells in our models, with granulocytic myeloid suppressor cells (G-MDSC) being the only cell type affected in the spleen (Supplementary Fig. 2); Zol reduced G-MDSCs under low concentrations of E2 ($p < 0.05$) in BALB/c mice and increased numbers of these cells under high concentrations of E2 in C57BL/6 mice.

Treatment with Zol predominantly altered the frequency of adaptive immune cells. Under low E2 concentrations, mice treated with Zol showed a significantly increased frequency of both intra-splenic CD8+ ($p < 0.01$ 4T1 [BALB/c], $p < 0.05$ E0771 [C57BL/6]; Fig. 2a) and CD4 + T-cells ($p < 0.01$ 4T1 [BALB/c], $p < 0.05$ E0771 [C57BL/6]; Fig. 2b). Similar Zol-induced changes in splenic T-cell frequencies were observed under high E2 concentrations ($p = 0.18$ 4T1 [BALB/c], $p < 0.05$ E0771 [C57BL/6]; Fig. 2c, d), albeit, not achieving statistical significance in the 4T1 model (BALB/c), with respect to CD8 + T-cells. Treatment with Zol under both low and high E2 concentrations did not induce consistent changes in the frequency of either intra-splenic NK or dendritic cells (Fig. 2e–h). Interestingly, the magnitude of the Zol-induced changes in splenic T-cell frequencies was greatly reduced under high concentrations of E2 in the 4T1 model (BALB/c)(Fig. 2a–d). Although baseline T-cell frequencies were similar under both high and low E2 concentrations in this strain (Supplementary Fig. 2i–l). In the E0771 model (C57BL/6), despite the magnitude of the Zol-induced changes in T-cell frequency being slightly increased under high E2 concentrations, this was coupled with a significantly reduced baseline frequency of both CD8+ (1.4% high E2; 2.6% low E2 $P < 0.05$) and CD4 + T-cells (1.6% High E2; 4.1% Low E2; $P < 0.01$) (Fig. 2a -d). Collectively, these data suggest that changes in E2 concentration alter the anti-metastatic efficacy of Zol by modulating T-cell frequency. These data suggest that suppression of T cells by E2 may be an important component leading to inhibition of anti-tumor response to Zol in premenopausal patients.

E2 shapes organ-specific immune responses to Zol in metastatic soft tissue and bone

Zol exerts differential anti-tumor effects in soft tissues and bone under pre- and postmenopausal concentrations of E2. Previously published data have shown that Zol does not accumulate in tumors, therefore, it is unlikely that this drug exerts direct anti-tumor cytotoxicity[22]. As Zol increases systemic T cell populations (Fig. 2), we hypothesized that anti-tumor effects of Zol may be associated with changes in the immune landscape of the bone and soft tissue microenvironments. To understand which immune cell changes were associated with the reduced soft tissue metastasis in mice treated with Zol under low E2 conditions, we applied flow cytometric profiling of lung metastatic samples. Under low E2, Zol significantly increased the frequency of CD8 + T cells ($p < 0.05$ and $p < 0.05$ for 4T1 [BALB/c] and E0771 [C57BL/6], respectively), with a strong trend towards an increased frequency of CD4 + T cells, albeit not significant ($p = 0.06$ for 4T1 [BALB/c] and $p = 0.053$ for E0771 [C57BL/6]), in soft tissue metastases, compared with saline treated controls (Fig. 3a, b). These Zol-induced changes to the

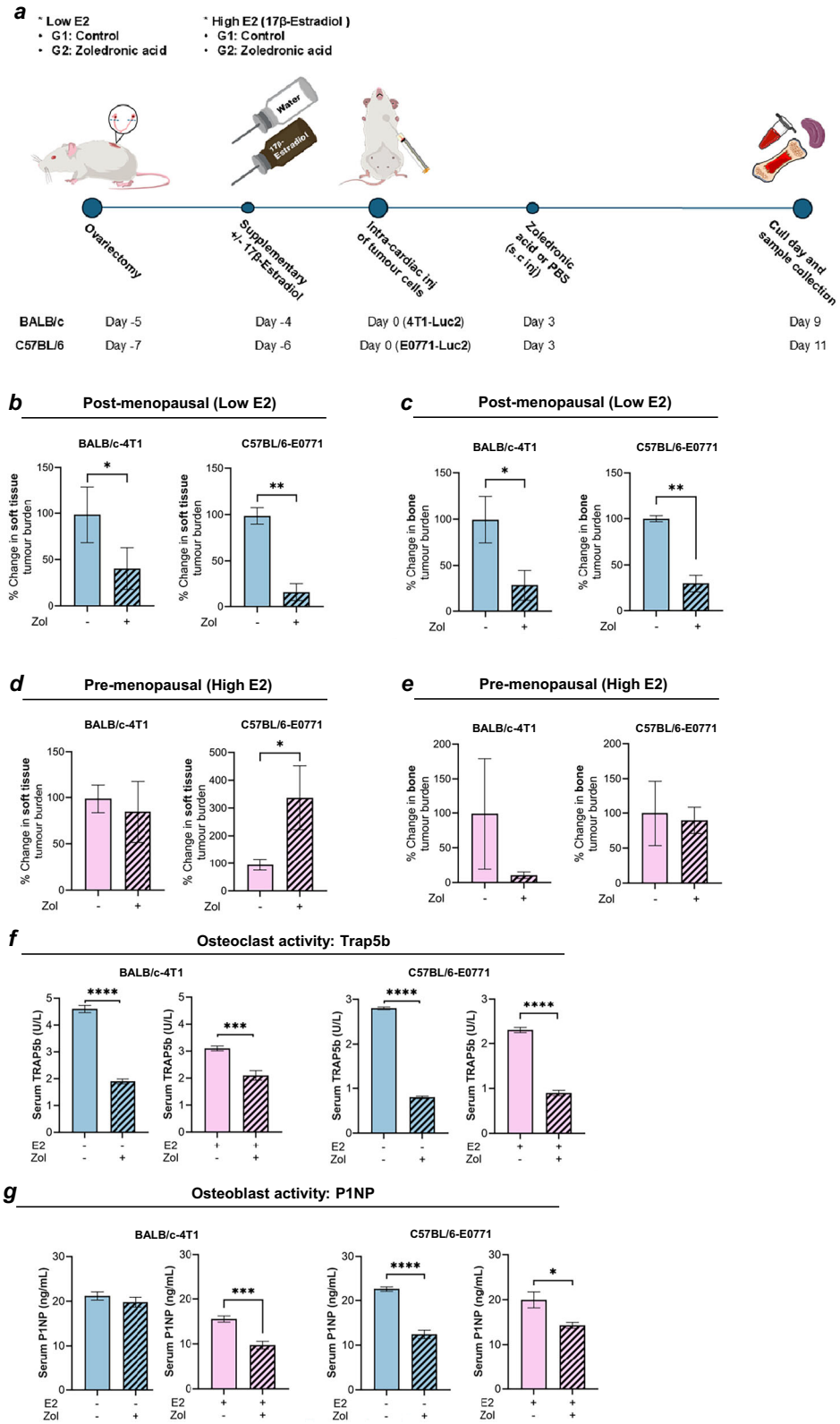


Fig. 1 | Effects of Zol on the metastatic outgrowth of tumor cells disseminated in bone and soft tissues in BALB/c and C57BL/6 mice under pre and postmenopausal concentrations of E2. BALB/c and C57BL/6 mice were ovariectomized followed by administration of E2/diluent in the drinking water to produce serum E2 concentrations equivalent to those found in pre and postmenopausal women. 4T1-luc2 or E0771-luc2 cells were administered via intracardiac injection 7-days after ovariectomy and mice treated with either PBS control or 100 μg/kg/week Zol 3-days later. **a** Schematic overview of the experimental protocol. % Change in tumor volume under low E2 conditions (postmenopausal) in soft tissues in (**b**) and in bone in (**c**). % Change in tumor volume in bone under high E2 conditions (premenopausal) in soft tissues in (**d**) and in bone in (**e**). Effects osteoclast and osteoblast activity as measured by serum concentrations of TRAP5b and P1NP are shown in (**f**, **g**), respectively. Data shown are mean +/− SEM, t test. $^{*}P < 0.05$; $^{**}P < 0.01$, $^{***}P < 0.001$, $^{****}P < 0.0001$.

metastatic lung immune landscape were not observed in high E2 conditions (Fig. 3c, d). Zol did not alter the frequency of innate immune cell populations in lungs affected by metastasis under either high or low E2 conditions (Fig. 3e–h and Supplementary Fig. 3). Taken together, these data suggest that under low E2 (as in postmenopausal women), Zol increases the frequency of CD8+ and CD4 + T cells in soft tissue tumors, like lung, and this is associated with reduced metastatic burden. However, the increased representation of CD8+ and CD4 + T cells in Zol-treated soft tissue tumors is absent under high E2 (as in premenopausal women) and is associated with enhanced tumor growth. These data indicate that CD8 + T cells are likely to be important for mediating the differential anti-tumor effects of Zol observed under varying concentrations of E2.

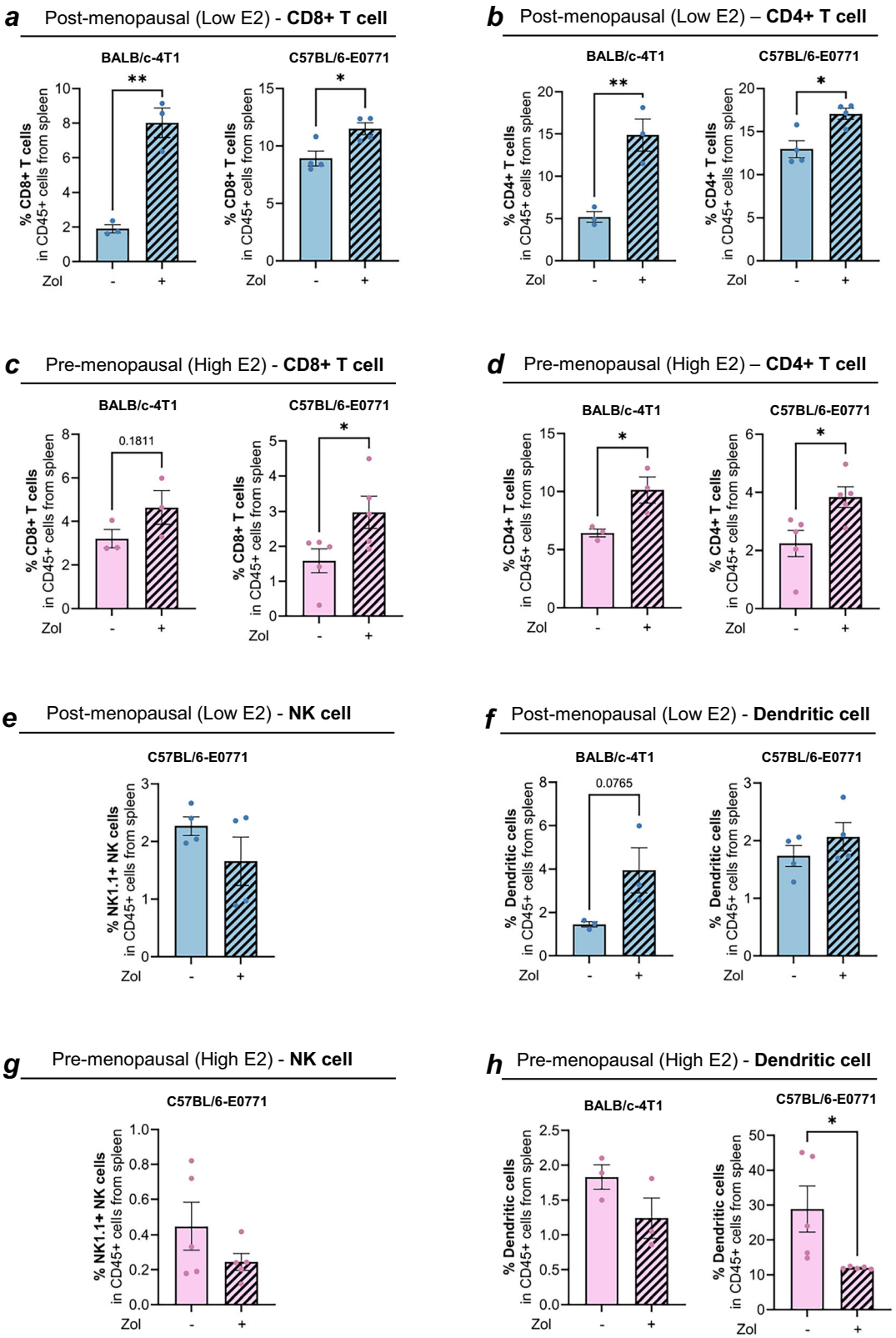


Fig. 2 | Effects of Zol +/− E2 on splenic immune cell populations isolated from BALB/c and C57BL/6 mice. BALB/c and C57BL/6 mice were ovariectomized followed by administration of E2/diluent in the drinking water to produce serum E2 concentrations indicative of those found in pre and post-menopausal women. 4T1-luc2 or E0771-luc2 cells were administered via intracardiac injection 7-days post ovariectomy and mice treated with either PBS control or 100 µg/kg/week Zol 3-days later. Spleens were dissected 9 and 11 days after injection of 4T1-luc2 or E0771-luc2 cells, respectively, and immune cell populations analyzed. Effects of Zol on CD8 + T and CD4 + T cells, are shown for low E2 conditions (postmenopausal) (**a**, **b**) and under high E2 conditions (premenopausal) (**c**, **d**). Effects on NK and dendritic cells are shown for low E2 conditions (postmenopausal) (**e**, **f**) and under high E2 conditions (premenopausal) (**g**, **h**). Data are mean +/− SEM, t test. $^{*}P < 0.05$; $^{**}P < 0.01$.

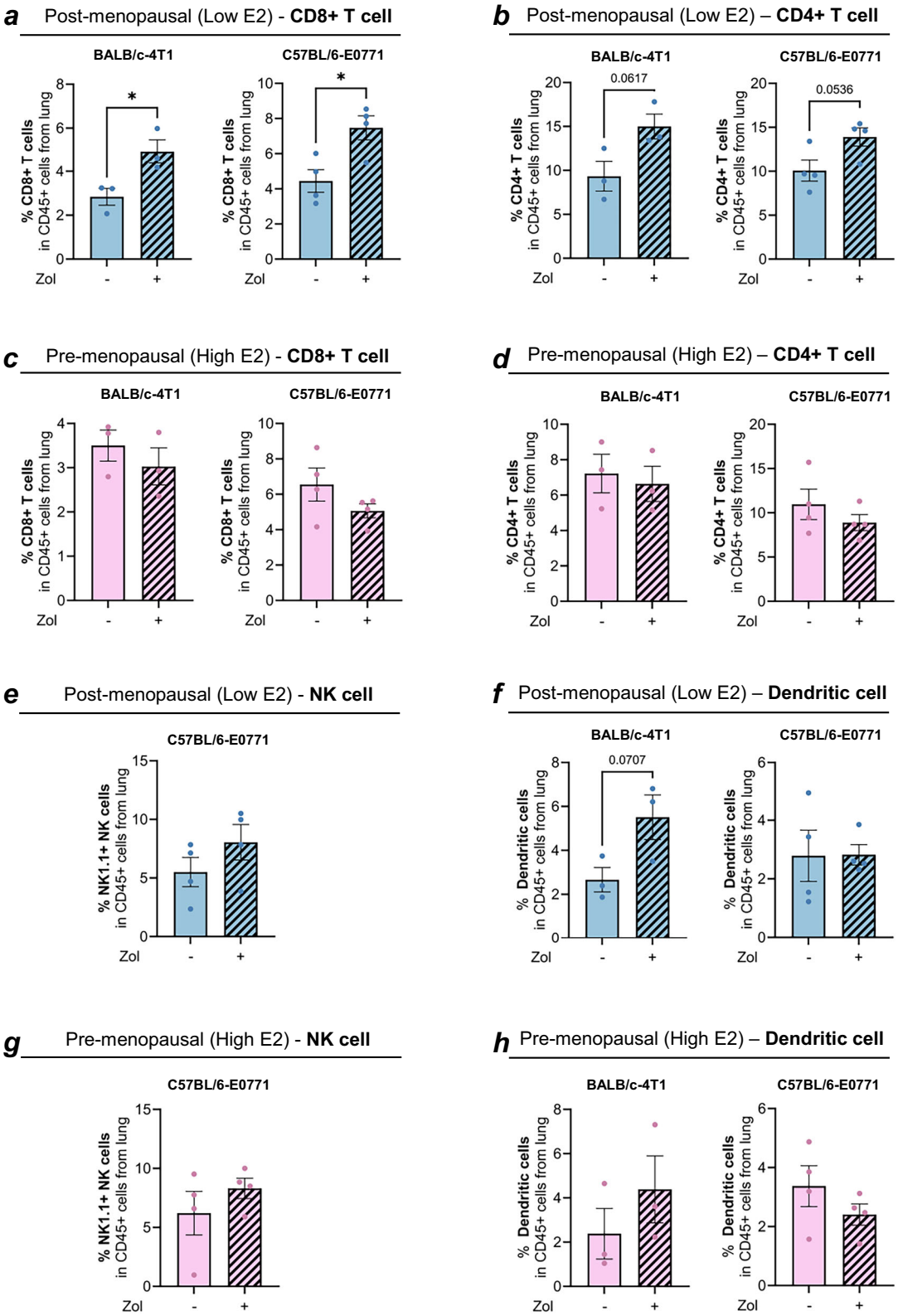


Fig. 3 | Effects of Zol on immune cell landscape in tumor-bearing lungs in BALB/c and C57BL/6 mice under pre and postmenopausal concentrations of E2. BALB/c and C57BL/6 mice were ovariectomized followed by administration of E2/diluent in the drinking water to produce serum E2 concentrations indicative of those found in pre- and postmenopausal women. 4T1-luc2 or E0771-luc2 cells were administered via intracardiac injection 7-days post ovariectomy and mice treated with either PBS control or 100 µg/kg/week Zol 3-days later. Tumor bearing lungs were dissected 9 and 11 days after injection of 4T1-luc2 or E0771-luc2 cells, respectively, and immune cell populations analyzed. Effects of Zol on infiltration of CD8 + T and CD4 + T cells into tumor bearing lungs, are shown for low E2 conditions (postmenopausal) (**a**, **b**) and under high E2 conditions (premenopausal) (**c**, **d**). Effects on NK and dendritic cells are shown for low E2 conditions (postmenopausal) (**e**, **f**) and under high E2 conditions (premenopausal) (**g**, **h**). Data are mean +/− SEM, t test. $^*P < 0.05$.

In both E0771 (C57BL/6) and 4T1 (BALB/c) metastatic bone environments, Zol treatment reduced metastatic burden (Fig. 1d) under low E2 conditions. Zol also significantly increased the frequency of both CD8 + T cells and macrophages (Fig. 4a-d), whilst reducing the frequency of pro-tumor G-MDSC cells (Fig. 4e). Thus, further suggestive that an immune-mediated mechanism was responsible for the anti-cancer effects of Zol in bone. The frequencies of NK cells, Dendritic cells, Monocytes, and B-cells were largely unaffected by treatment with Zol (Supplementary Fig. 4a–h). Interestingly, the ability of Zol to reduce tumor burden in bone directly correlated with the increased frequencies of both T cells and macrophages in this environment when treated with Zol: In the 4T1 model (BALB/c), where Zol reduced tumor burden in bone, regardless of E2 concentrations, Zol increased the frequencies of CD8+ and CD4 + T cells, and macrophages (Figs. 1d, e and 4a, d, e, h). In contrast, in the E0771 model (C57BL/6) exposed to high E2, where Zol was unable to alter bone tumor burden, Zol failed to elicit CD8 + T cells, CD4 + T cells, or macrophages (Figs. 1e and 4e, f, h). These data further point towards modulation of T-cell representation, and possibly their activity, as important mechanisms underlying the anti-metastatic activity of Zol under different E2 concentrations.

E2 impedes anti-cancer immunity through reducing NK cells and increasing expression of immune checkpoint inhibitors

Our existing data suggested that E2 modulates the anti-tumor effects of Zol through an immune-mediated mechanism, thus we next investigated how the frequencies of key immune cell types were altered by E2 alone. In both E0771 (C57BL/6) and 4T1 (BALB/c) models, E2 did not significantly alter endpoint tumor burden (Fig. 5a, b). Although, there was a trend towards increased burden under high E2 conditions. However, high E2 was associated with reduced frequencies of splenic CD8+ and CD4 + T cells, and CD49b+ NK cells, most pronounced in the 4T1 model (BALB/c; Fig. 5c–e). The frequency of dendritic cells was unchanged (Fig. 5f). To determine whether E2 affected the anti-tumor activity of these immune cell populations, ex vivo co-culture experiments were performed. Co-culture of spleen-derived CD8 + T cells and NK cells isolated from 4T1 tumor-bearing mice exposed to high or low E2 with 4T1 cells demonstrated that E2 significantly reduced the tumoricidal activity of both CD8 + T-cells and NK cells (Fig. 5g). E2 did not affect other innate immune cells in our models (Supplementary Fig. 5a–d).

The tumoricidal activity of T and NK cells is influenced by complex factors within the tumor microenvironment; key among these are immune checkpoints, acting both systemically during priming and locally at the tumor site. Flow cytometric analysis revealed a significant increase in the frequencies of programmed death protein 1 positive (PD-1) intra-splenic NK cells (Fig. 6a), peripheral blood NK and CD8 + T cells (Fig. 6b), and CD4+ and CD8 + T cells in tumor-bearing lungs (Fig. 6d), but not in bone (Fig. 6e) or mice exposed to high E2 relative to low E2. Furthermore, isolation of primary E0771 tumors from E2 treated and control mice demonstrated an increase in expression of the PD-1 ligand (protein death ligand 1; PD-L1) in tumors exposed to a high E2 environment (Fig. 6e and Supplementary Fig. 5f). Because the functional role of PD-1 is highly context-dependent, being upregulated during both early T-cell activation and exhaustion, we reasoned that concurrent elevation of PD-1 and PD-L1 could create an environment permissive to checkpoint-mediated suppression. Together, these data suggest that under premenopausal concentrations of E2, T cells and NK cells frequencies are not only reduced but, their capacity to control soft-tissue tumor growth may be further constrained by heightened PD-1/PD-L1 mediated suppression. In addition, splenic CD69 + NK, CD8+ and CD4 + T cells were decreased and CD27 + NK and CD8 + T cells increased in E2 high environments (Fig. 6g, h). Taken together these data suggest that high E2 inhibits anti-tumor efficacy of T and NK cells by reducing their frequency and activity, possibly through the PD-1/PD-L1 axis in soft tissues.

Analyzing tumor samples from patients enrolled in the AZURE trial, we found significantly higher levels of PD-L1 expression in premenopausal compared to peri- ($p = 0.0022$) and postmenopausal ($p = 0.018$) women (Fig. 7a). Importantly, retrospective analysis of tumor samples from AZURE patients revealed a significant correlation between PD-L1 expression in primary tumors and reduced efficacy of Zol: Expression of PD-L1 did not alter disease free survival (Fig. 7b), overall survival (Fig. 7c) or recurrence at any site (Fig. 7d, e) in patients treated with standard of care alone. However, patients with PD-L1- tumors benefitted significantly from addition of Zol to standard of care, having increased disease-free survival ($p = 0.0052$; Fig. 7b), increased overall survival ($p = 0.029$; Fig. 7c), reduced recurrence in bone ($p = 0.019$; Fig. 7d), reduced recurrence in soft tissue ($p = 0.032$; Fig. 7e) and reduced distant recurrence ($p = 0.0019$; Fig. 7f). These data strongly support our hypothesis that the increased expression of immune checkpoints under high E2 concentrations prevents Zol from exerting its anti-tumor effects.

Organ-specific immune cell dependencies govern anti-tumor efficacy of Zol

To establish which cells were most important in enabling Zol to exert anti-tumor effects under low E2 conditions, CD8 + T cell and NK cell antibody depletion experiments were performed in ovariectomized C57BL/6 mice (Fig. 8a) and NK-cell and $CD8^+$ T-cell depletion efficiencies were validated by antibody treatment (Supplementary Fig. 6). In our model, depletion of NK but not CD8 + T cells significantly increased tumor growth (Fig. 8b, c) and reduced metastasis-free survival (Fig. 8d). Depletion of CD8 + T cells did not affect the ability of Zol to reduce tumor growth or increase survival (Fig. 8e, f), whereas depletion of NK1.1 cells inhibited the ability of Zol to reduce tumor growth (Fig. 8g) and resulted in reduced metastasis free survival (Fig. 8h). The ability of Zol to inhibit bone metastasis appeared to be entirely dependent on the presence of NK cells (Fig. 8i). In soft tissue (lung), both NK cells and CD8 + T cells appear to be important in Zol-driven anti-tumor immunity, as Zol did not exert anti-tumor effects in this site without the presence of both cell types (Fig. 8j).

Combining Zol with PD-L1 or PD-1 inhibition increases the anti-tumor effects of Zol in soft tissue and bone

Our data demonstrate that Zol exerts anti-tumor activity via both NK and CD8 + T-cells in soft tissue but relies solely on NK cells in bone (Fig. 8). We have also shown that the proportion of T-cells and NK cells expressing the immune checkpoint PD-1 and the level of PD-L1 expressed within primary tumors (Fig. 6) are elevated under high E2 conditions. Furthermore, that PD-L1 expression correlates with poor response to Zol in clinical samples (Fig. 7). We therefore performed additional experiments to determine whether this co-upregulation of PD-1 and PD-L1 constitutes a functional inhibitory axis that limits the anti-tumor efficacy of Zol using blocking antibodies. Combining Zol with a PD-L1 blocking antibody (Fig. 9a) significantly reduced soft tissue metastasis under high E2 concentrations (Fig. 9b, ci and Supplementary Fig. 7). Similar results were obtained when a neutralizing antibody against PD-1 was given in combination with Zol (Fig. 9d–f). Flow cytometric profiling of the intra-splenic immune landscape revealed the combination therapy significantly increased the frequency of both CD4+ and CD8 + T-cells, while simultaneously decreasing the frequency of regulatory T-cells (Fig. 10a–c). The remaining leukocyte populations - including B-cells, NK-cells, MDSCs, DCs, macrophages and monocytes—showed no biologically meaningful change in response to combination therapy (Fig. 10d–i). Taken together, these data indicate that targeting the PD-1/PD-L1 immune checkpoint successfully rescues Zol efficacy in soft tissues under high E2 conditions. Importantly, Zol renders anti-PD-1/PD-L1 therapies effective at treating metastases in the context of high estrogen.

Discussion

Adding adjuvant bisphosphonate to standard of care therapy for the prevention of distal recurrence in postmenopausal breast cancer patients has been widely adopted in the UK and Europe and is recommended in international consensus guidelines[4,23,24]. Understanding why bisphosphonates do not provide the same anti-tumor benefits in premenopausal women is

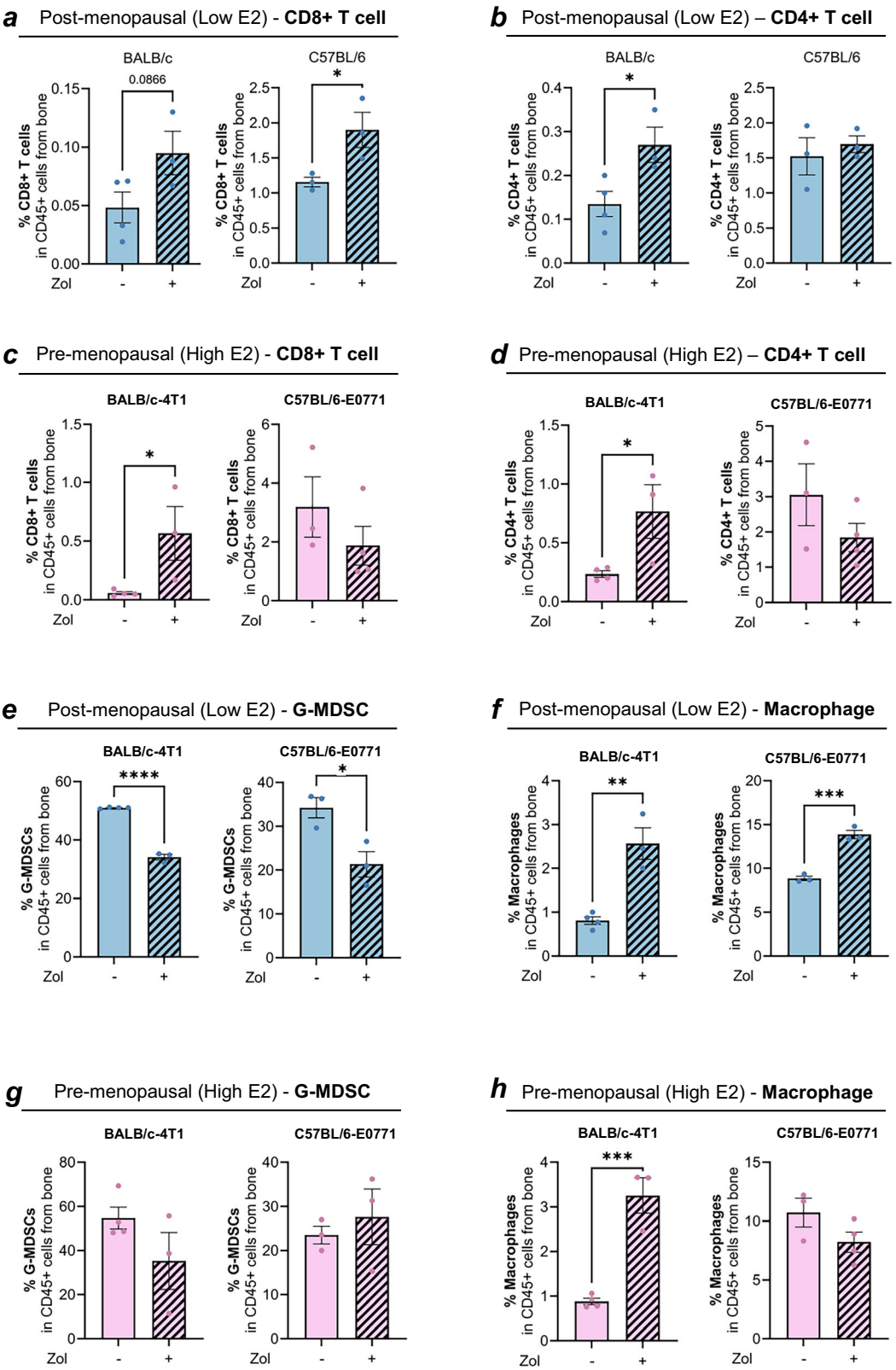


Fig. 4 | Effects of Zol on immune landscape in tumor-bearing bone in BALB/c and C57BL/6 mice under pre and postmenopausal concentrations of E2. BALB/c and C57BL/6 mice were ovariectomized followed by administration of E2/diluent in the drinking water to produce serum E2 concentrations indicative of those found in pre- and postmenopausal women. 4T1-luc2 or E0771-luc2 cells were administered via intracardiac injection 7-days post ovariectomy and mice treated with either PBS control or 100 µg/kg/week Zol 3-days later. Tumor bearing bones were dissected 9 and 11 days after injection of 4T1-luc2 or E0771-luc2 cells, respectively, and immune cell populations analyzed. Effects of Zol on immune cell populations in bone tumors **a** CD8 + T cells, **b** macrophages, **c** G-MDSCs, and **d** CD4 + T cells are shown under low E2 conditions (postmenopausal) Effects of Zol on immune cell populations in bone tumors **e** CD8 + T cells, **f** macrophages, **g** G-MDSCs, and **h** CD4 + T cells are shown under high E2 conditions (pre-menopausal). Data are mean +/− SEM, t test. $^{*}P < 0.05$, $^{**}P < 0.01$, $^{***}P < 0.001$, $^{****}P < 0.0001$.

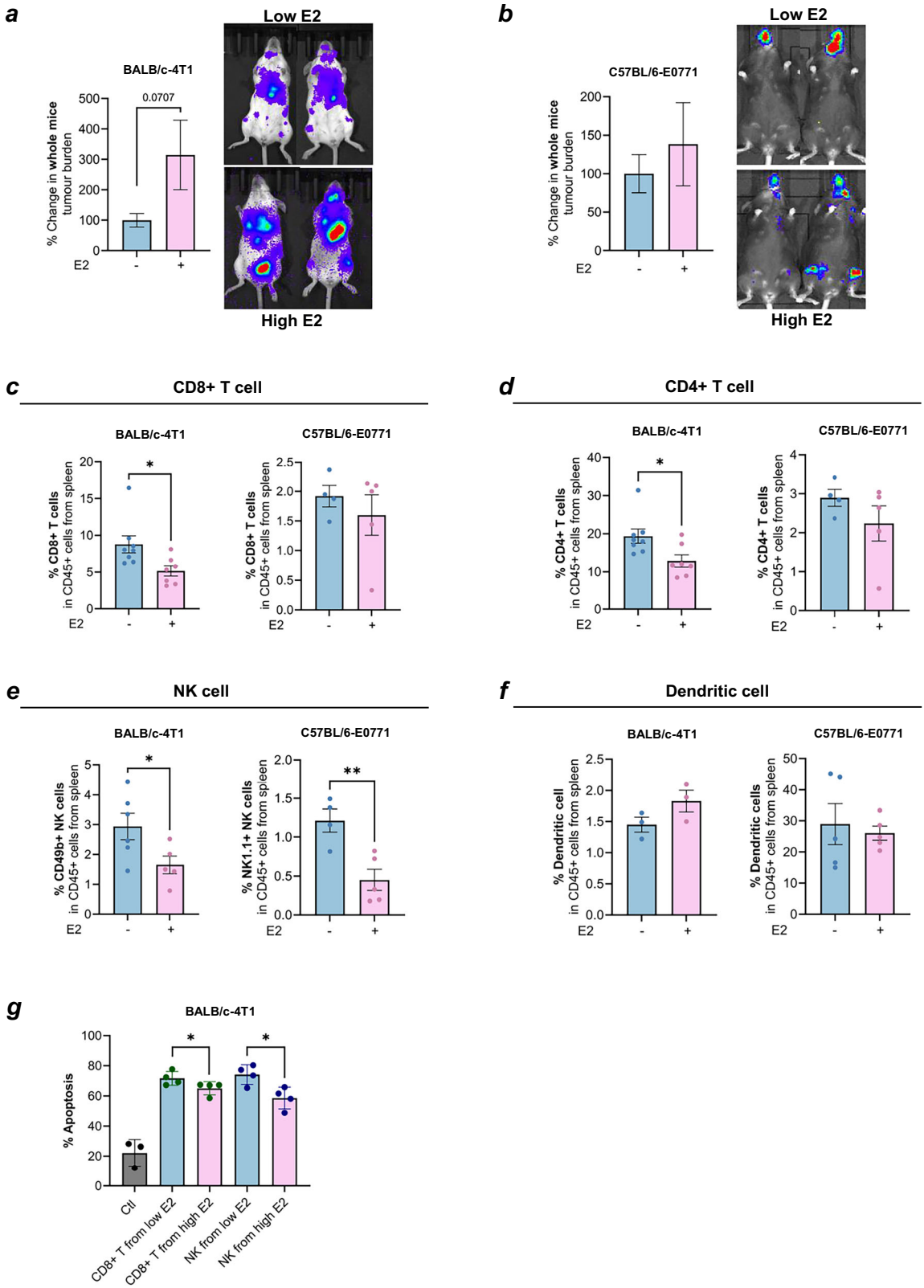


Fig. 5 | Estrogen reduces the frequencies and anti-tumor activity of NK and T cell populations. BALB/c and C57BL/6 mice were ovariectomized followed by administration of E2/diluent to produce serum E2 concentrations complementary of those found in pre- and postmenopausal women. 4T1-luc2 or E0771-luc2 cells were administered via intracardiac injection 7-days after ovariectomy. % Change of tumor volume, in whole mice, and representative IVIS images are shown in (**a**) for BALB/c mice injected with 4T1-luc2 cells and **b** for C57BL/6 mic injected with E0771-luc2 cells. Effects of E2 on splenic immune cell populations in these mice are shown for **c** CD8 + T cells, **d** CD4 + T cells, **e** NK cells, and **f** Dendritic cells. Apoptosis assays from co-cultures of 4T1-luc2 cells with CD8 + T cells and NK cells, isolated from BALB/c spleens, were assessed to determine tumor killing capabilities of these cell types; % Apoptosis of is shown in (**g**). Data are mean +/− SEM, t test. *P < 0.05, **P < 0.01, ***P < 0.001.

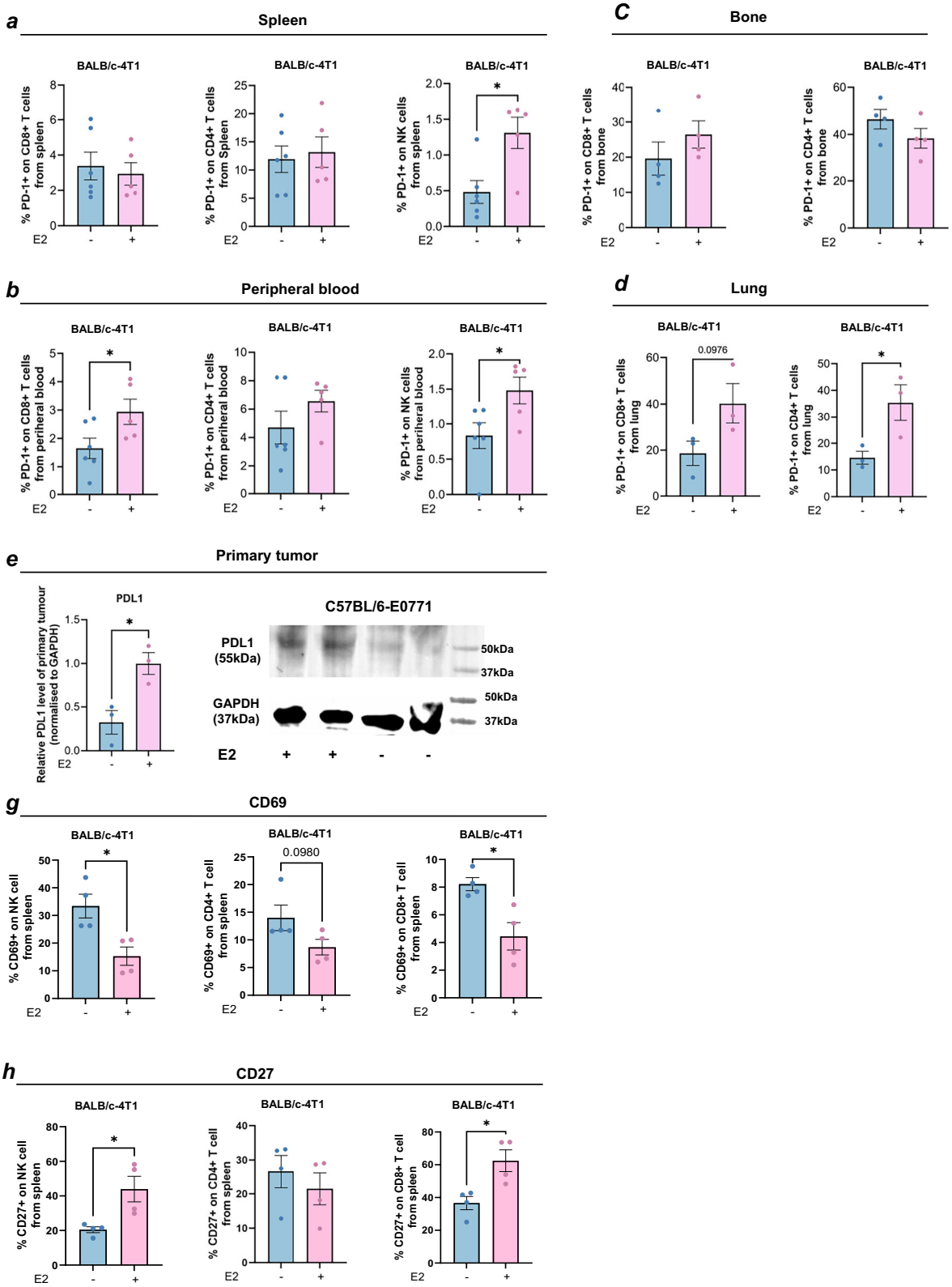


Fig. 6 | Increased proportion of immune checkpoint positive NK and T cells under high E2 conditions. BALB/c and C57BL/6 mice were ovariectomized followed by administration of E2/diluent in the drinking water to produce serum E2 concentrations indicative of those found in pre- and post-menopausal women. 4T1-luc2 or E0771-luc2 cells were administered via intracardiac injection or intra-ductal (mammary duct) injection 7-days post ovariectomy and mice treated with either PBS control or 100 µg/kg/week Zol 3-days later. Primary tumors were removed 15 days after tumor cell injection and, whole blood, spleens, tumor bearing lungs and bones were dissected 9 and 11 days after injection of 4T1-luc2 or E0771-luc2 cells, respectively. PD-1 expression was measured on CD4+ and CD8 + T and NK cells via flow cytometry in the spleen (**a**) peripheral blood (**b**) bone marrow (**c**) and lung (**d**) from BALB/c mice. PD-L1 expression measured on E0771-luc2 primary tumors by Western blot (**e**). Data shown are mean +/− SEM, t test. $^*P < 0.05$.

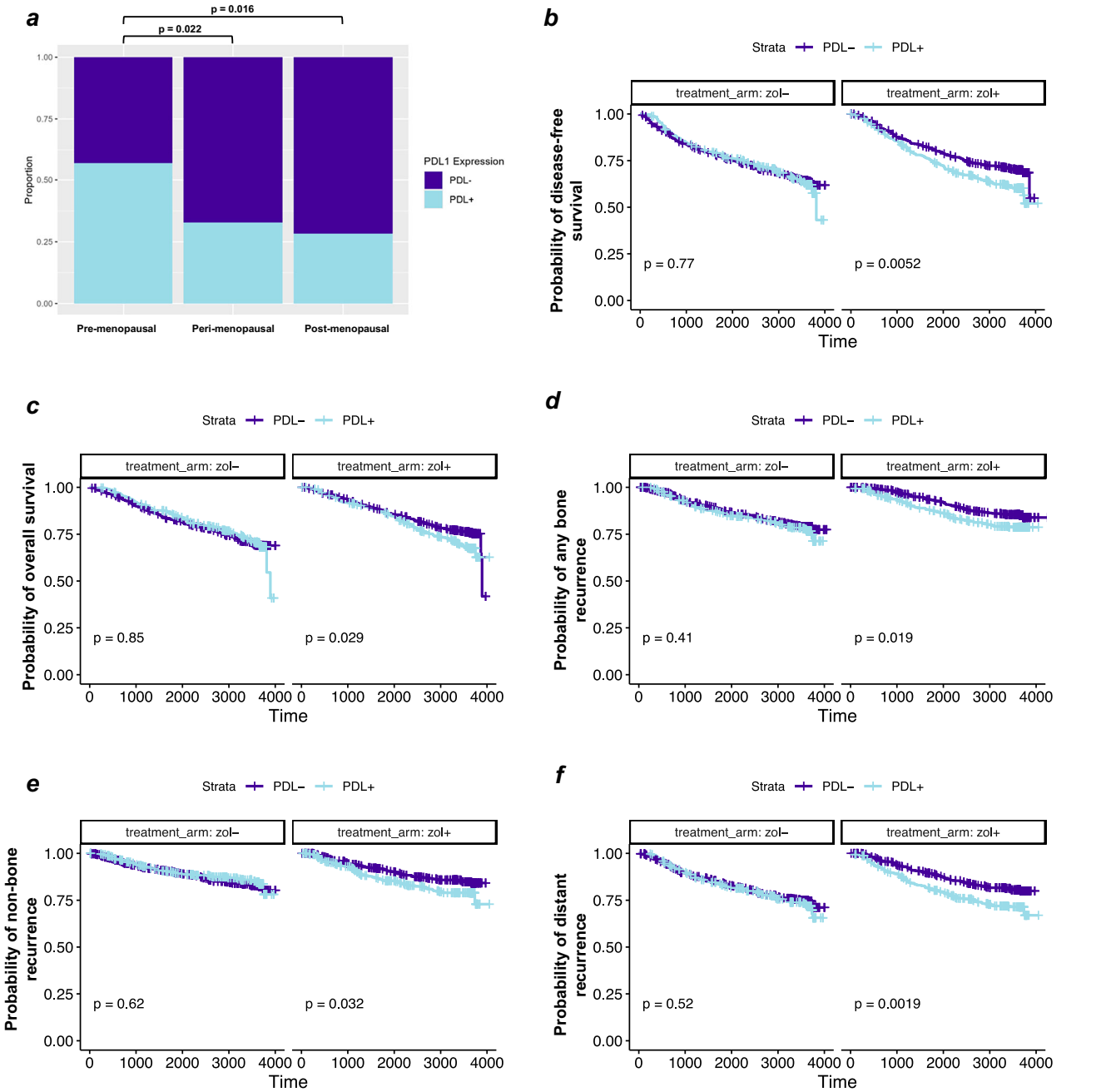


Fig. 7 | PD-L1 expression correlates with menopause and improved survival following adjuvant Zol in breast cancer patients. PD-L1 expression was assessed on tissue microarrays containing 3-separate primary tumor cores/patient from 1,729 patients included in the clinical trial AZURE. All patients included had menopausal biochemically confirmed prior to data analysis. Correlation between PD-L1 expression on tumors and menopausal status are shown in (**a**). Correlation between PD-L1 expression and patient outcome following treatment with standard of care or standard of care with the addition of Zol are shown in terms of disease-free survival (**b**), overall survival (**c**), tumor recurrence in bone (**d**), tumor recurrence outside of bone (soft tissue) (**e**), and distant recurrence **f**).

crucial if we are to find better outcomes for the 460,000 young women who develop this disease every year[2]. Using serum samples from the AZURE trial, we have previously shown an association between E2 levels of ≥50 pmol/l (premenopausal range) and significantly shorter invasive disease-free survival, compared to oestradiol levels of <50 pmol/l (HR = 1.36; 95% CI 1.05–1.78 $p = 0.022$)[1,16]. Shorter disease-free survival was driven by more distant recurrences (outside of bone), irrespective of whether the primary tumor was estrogen receptor positive or negative. In our current study, we have focused on elucidating the effects of Zol using two syngeneic mouse model—a model of triple-negative breast cancer (4T1) and a model of luminal-B-like (E0771)—representing two aggressive subtypes enriched in premenopausal women and where improved treatments are urgently needed[25]. We successfully modeled the effects of Zol in BALB/c and C57BL/6 mice using significantly different E2 concentrations comparable to those found in pre- and postmenopausal patients(<50 pmol/L associated with reduced distal recurrences or >50 pmol/L associated with increased distal recurrences following Zol), though the precise serum concentrations were strain-dependent, thereby recapitulating the distinct endocrine environments evaluated in the AZURE trial. These syngeneic models were selected because they capture distinct combinations of intrinsic tumor biology and host immune background, better reflecting the heterogeneity observed in human breast cancer. At the tumor level, the 4T1 (BALB/c) and E0771

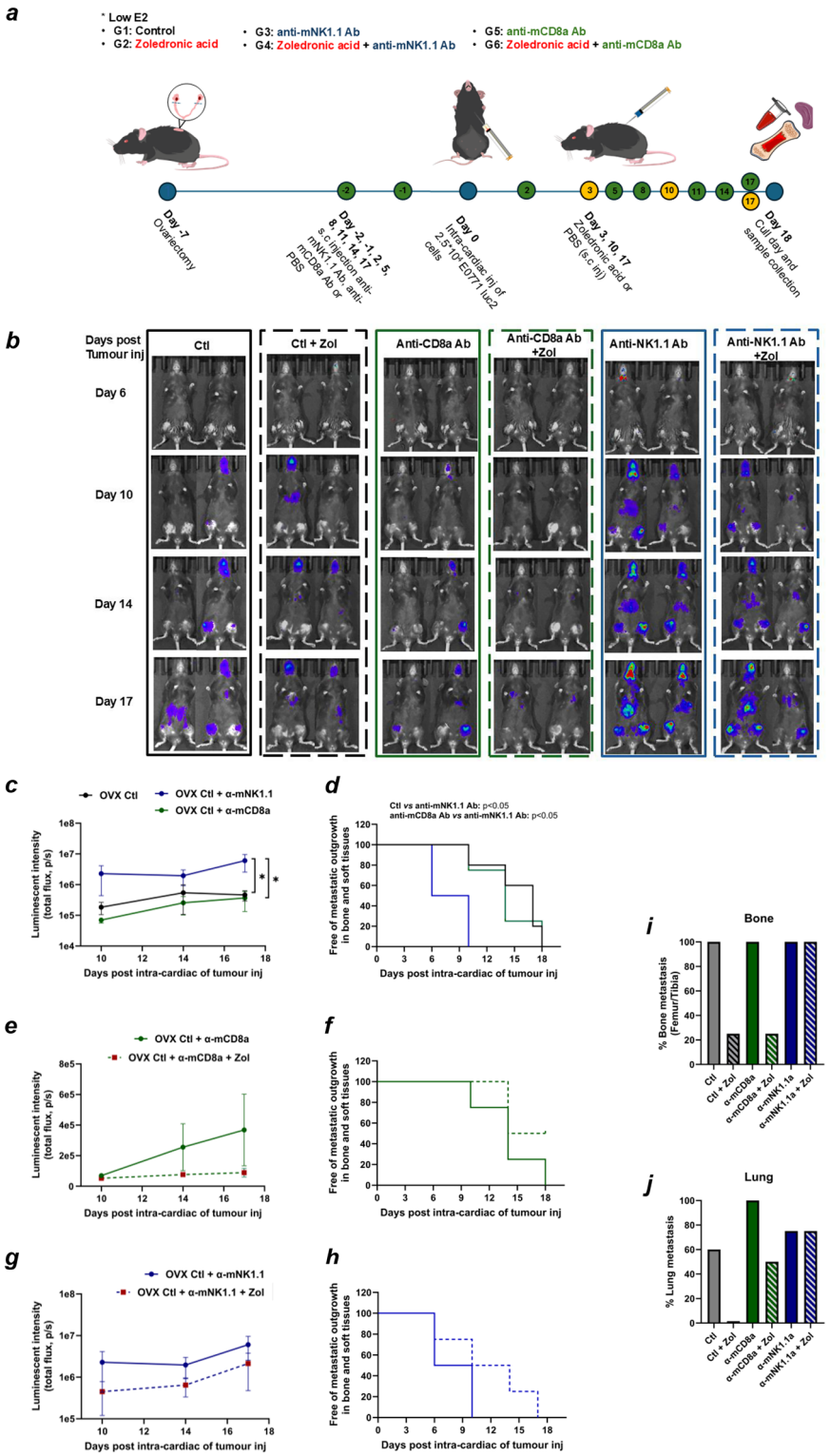


Fig. 8 | NK cells depletion prevents Zol induced anti-tumor effects. Postmenopausal concentrations of E2 were modeled in 12-14 week old female C57BL/6 mice. 5-days later mice were subject to antibody depletion of NK1.1 cells or CD8 + T cells and E0771-luc2 cells were administered by intra-cardiac injection 2-days after the first antibody injection. Mice were administered 100 µg/kg/week Zol or PBS control 3-days later and development of metastases analyzed over 18 days. **a** Schematic overview of the experimental protocol. **b** Representative whole body IVIS images of mice at Day 6, Day 10, Day 14, and Day 17 post intracardiac injection of E0771 luc2. **c** Quantification (photons/sec (p/s) of tumor growth of whole mice and **d** percent of mice free of metastatic disease following NK1.1 or CD8 + T cell depletion. **e** Quantification (photons/sec (p/s) of tumor growth in whole mice and **f** Percent of mice free of metastatic disease following CD8 T cell depletion +/− Zol treatment. **g** Quantification (photons/sec (p/s) of tumor growth of whole mice and **h** % of mice free of metastatic disease following NK1.1 cell depletion +/− Zol. **i** Percent of mice that developed bone metastases and **j** Percent of mice that developed lung metastasis following NK1.1 or CD8 + T cell depletion +/− Zol. Data are mean +/− SEM with statistical significance determined by two-way ANOVA with Tukey's post doc. $^*P < 0.05$.

(C57BL/6) lines represent distinct molecular and clinical subtypes—differing estrogen receptor status, growth kinetics, intrinsic immunogenicity, and metastatic propensity. At the host level, BALB/c and C57BL/6 inbred strains exhibit marked differences in baseline immune bias: C57BL/6 mice preferentially mount a Th1-dominated response driven by IFNG, whereas BALB/c mice are biased toward a Th2 response and B-cell humoral immunity[26]. Moreover, C57BL/6 mice express higher baseline levels of immune checkpoints compared to BALB/c mice[27]. Evaluating both the 4T1 and E0771 systems thus enabled us to investigate how Zol and E2 regulate anti-tumor immunity across divergent tumor microenvironments and immunological baselines.

The effects of Zol on tumor growth in soft tissue mirrored data from clinical breast cancer trials: In BALB/c mice, Zol reduced metastasis under low E2 and increased metastasis under high E2 (similar to the AZURE trial)[1]; in C57BL/6 mice, Zol reduced metastasis under low E2 and did not affect metastasis under high E2 (similar to the ABCSG-12 trial)[12]. Our data demonstrate that under low E2, the anti-tumor effects of Zol are dependent on CD8 + T and NK cells, as antibody depletion of these cells results in the

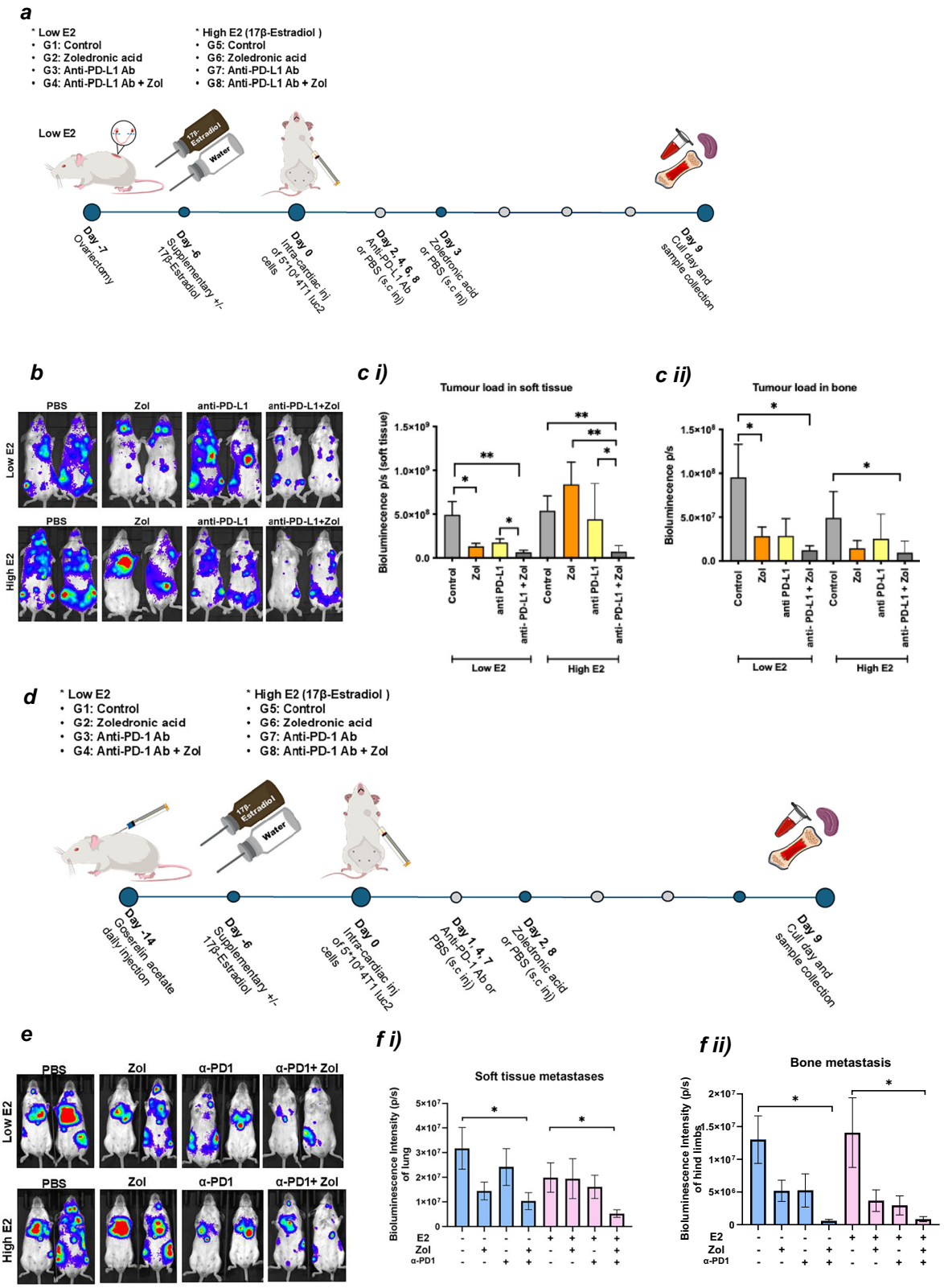


Fig. 9 | Inhibition of PD-L1 or PD1 increases the anti-tumor effects of Zol in soft tissues. Pre- and postmenopausal concentrations of E2 were modeled in 12–14 week old female BALB/c mice 7-days prior to receiving an intracardiac injection of 50,000 4T1-luc2 cells. PBS/control or 30 mg/kg mouse anti-PDL-1 antibody was administered every two days or 250 µg/mouse, mouse anti-PD-1 administered every 3-days starting 2-days after tumor cell injection followed 24 h later by 100 µg/kg/week Zol or PBS control. Mice were culled 9 days after tumor cell injection as indicated in (**a**) the experimental outline for experiments utilizing anti-PD-L1. **b** Shows representative whole body IVIS images of mice 8-days post tumor injection. **ci** Shows quantification of tumor burden in soft tissues measured in p/s and **cii** shows qualification of tumor burden in bone (p/s). **d** Shows the experimental outline for experiments using anti-PD-1. **e** Shows representative whole body IVIS images of mice 8-days post tumor injection. **fi** Shows quantification of tumor burden in soft tissues measured in p/s and **fii** shows qualification of tumor burden in bone (p/s). Data are mean +/− SEM with statistical significance determined by two-way ANOVA with Tukey's post doc test. $^{*}P < 0.05$, $^{**}P < 0.01$.

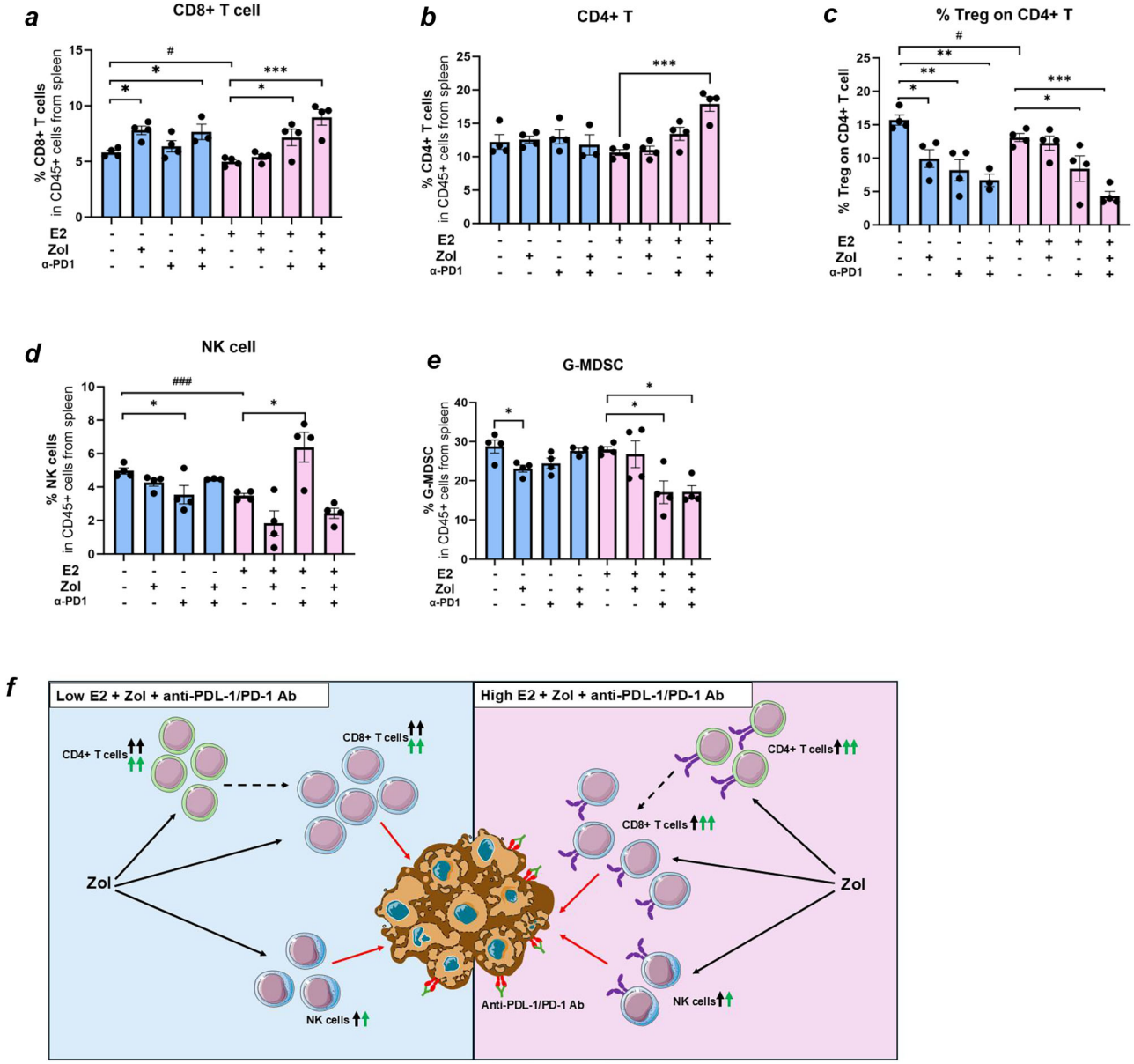


Fig. 10 | Effects of combining a PD-1 neutralizing antibody with Zol under +/- on systemic immune cell populations isolated from BALB/c mice. Pre- and post-menopausal concentrations of E2 were modeled in 12–14 week old female BALB/c mice 7-days prior to receiving an intracardiac injection of 50,000 4T1-luc2 cells. Mice received 250 µg/mouse/3-days anti- mouse PD-1 antibody, 100 µg/kg/week Zol, PBS control, or combination therapy. Spleens were dissected 9 days after injection, and immune cell populations were analyzed. Effects of treatments on immune populations are shown: CD8 + T in (**a**), CD4 + T in (**b**), Treg in (**c**), NK in (**d**), and G-MDSC in (**e**). Data are mean +/− SEM, with statistical significance determined by two-way ANOVA with Tukey's post doc or t test. $^{*}P < 0.05$, $^{**}P < 0.01$, $^{***}P < 0.001$.

loss of anti-tumor activity. Whether Zol acts directly on these effector lymphocytes, indirectly through broader reprogramming of the tumor immune microenvironment, or a combination of both remains to be fully elucidated. Zol has previously been shown to have immune stimulatory effects in the context of cancer progression, switching macrophage polarization towards an anti-tumor phenotype, increasing gamma-delta T cell activation, decreasing Treg cell proliferation and activation, and increasing NK cell peripheral expansion (reviewed in ref. 21). However, many of these studies have been performed using immune cells isolated from mice and/or humans with unknown E2 levels (likely low; from mice with ~ 17–62 pg/ml serum E2 or postmenopausal osteoporosis patients treated with Zol). The interactions between E2 and Zol have not previously been investigated. In soft tissue metastasis under low E2, we did not see a change in either macrophage polarization or numbers and, with the exception of monocytes, the frequencies of innate immune cells did not appear to be affected by Zol; therefore, we did not investigate this further. It is likely that the increased numbers of CD8+ and CD4 + T cells observed are the result of Zol reducing Tregs. Although we did not see a significant change in the numbers of NK cells following Zol, there was a trend towards increased numbers in soft tissue. Ex vivo, co-culture using CD8 + T and NK cells isolated from hosts exposed to high E2 demonstrated impaired anti-tumor effector activity. These findings indicate that E2-mediated suppression of the Zol-induced response likely involves reductions in both effector cell function and frequency. It should be noted that BALB/c and C57BL/6 mice express different NK cell populations, with NK 1.1 cells present in C57BL/6[28] and less mature CD49b+ NK cells in BALB/c mice[29]. Our current data suggest that both NK cell subtypes are required during Zol-mediated suppression of metastases in soft tissue.

The vast majority of information relating to the effects of E2 on immunity has been identified in the context of infection and inflammation-related conditions. In these contexts, E2 has been shown to have immune suppressive effects including switching macrophage polarization towards an inflammatory phenotype, decreasing T lymphocyte development and activity, and decreasing the cytotoxic actions of NK cells[26,30–34]. Original research relating to effects of E2 on anti-cancer immunity is scarce, with most review articles extrapolating information from other disease types. Information associated with the effects of E2 on immune checkpoint expression in cancers is contradictory, with evidence from lung cancers and estrogen receptor positive breast cancer cell lines suggesting that E2 may upregulate PD-L1 on tumors, helping them to evade immune response[35,36]. A more recent study demonstrated reduced PD-L1 expression on estrogen receptor positive cells following exposure to E2[37]. Differences in reporting may be due to whether the gene coding PD-L1, *Cd274*, is regulated via genomic or non-genomic mechanisms. In small cell lung cancer, focal gene amplifications and copy number gains in chromosome 9p24, on which *CD274* resides, have been reported, suggesting that PD-L1 expression in this cancer type is regulated at a genome level[38]. In contrast, evidence suggests that *CD274* copy number variation is rare in breast cancers, instead, environmental factors, including presence of cytotoxic and regulatory T cells, have been proposed to regulate PD-L1 in ER negative breast cancers[39]. There is therefore an urgent need to better understand how the environment and E2 influence the immune landscape in cancers, including breast, as immune regulation impacts prognosis and treatment efficacy. In the setting of triple-negative breast cancer, our data demonstrate reduced CD8 + T cells, CD4 + T cells, and NK cells under high concentrations of E2, confirming what others have found in different disease settings[40–42]. Furthermore, we demonstrate increased expression PD-L1 on tumor cells and increased expression of the checkpoint inhibitor PD1 on T cells and NK cells. Importantly, our data show that under high E2 Zol is unable to exert anti-tumor effects in soft tissue, as it is unable to elicit T cell responses to levels seen under low E2. Elevated PD-L1 on tumor cells and PD-1 on T and NK cells under high E2 conditions prevents immune-mediated control of tumor growth. These data are in agreement with patient-derived data demonstrating increased PD-L1 in premenopausal compared to post-menopausal patients and a strong correlation between PD-L1 expression and poor anti-tumor response to Zol (Fig. 7).

It has previously been postulated that bisphosphonates, including Zol, exert anti-tumor effects in bone by inhibiting osteoclast activity, reducing bone turnover and disrupting the "vicious cycle" of bone metastases[43–45]. However, there is increasing evidence suggesting that inhibition of osteoclast activity, alone, is not sufficient to prevent development of metastasis in this site. For example, the RANKL-targeted antibody, denosumab that prevents maturation of pre-osteoclasts into osteoclasts, is significantly more potent at reducing osteoclast activity compared with bisphosphonates. However, denosumab does not prevent recurrence of breast tumors in bone, nor does this treatment alter disease-free or progression-free survival in either pre- or postmenopausal women[46,47]. Our new data strongly suggest that immune cell regulation is key to the anti-metastatic effects of Zol in bone. Administration of Zol resulted in increased frequencies of dendritic cells, CD8+ and CD4 + T cells, and macrophages in the bone micro-environment, as well as reduced G-MDSC cells. G-MDSCs have recently been implicated in pro-tumor activities, stimulating the growth of tumor cells[48,49]. This cell type may, therefore, be important in supporting Zol-induced anti-tumor activity, and failure to reduce G-MDSCs under high E2 may, in part, be responsible for the reduced anti-tumor responses to Zol seen in premenopausal women. Interestingly, in BALB/c mice, where bone metastasis was reduced under both high and low E2, the frequencies of CD8+ and CD4 + T cells in bone were elevated in mice treated with Zol regardless of E2 levels. In contrast, in C57BL/6 mice, where Zol did not reduce bone metastasis under high E2, macrophages, CD4 + T cells, CD8 + T cells, and NK cells were unaltered following administration of Zol. This is an important finding, as not all patients exhibit reduced recurrence in bone following Zol, and understanding an immunological phenotype that is predictive of benefit could be developed into a biomarker to stratify likely responders from non-responders. Despite the data presented in Fig. 4 suggesting that T cells may be important in regulating the anti-tumor response to Zol in bone, depletion of CD8 + T cells has no effect on the ability of Zol to reduce metastasis at this site. Instead, activity of NK cells appears to be more important in bone, as Zol is unable to reduce metastasis in the absence of NK cells (Fig. 8). These data are in fitting with our previously published research showing that Zol inhibits bone metastasis in BALB/c nude mice that possess NK cells but not T cells[17].

In conclusion, we have demonstrated that Zol induces a CD8 + T-cell and NK cell-dependent anti-tumor response against soft tissue metastases. However, this response—along with the increased frequency of these effector cells at metastatic sites—occurs strictly under low E2 conditions characteristic of postmenopausal status. Interestingly, the anti-tumor response induced by Zol in bone is dependent only on NK cells. In high E2 conditions (as in premenopausal women), elevated circulating E2 is associated with decreased frequencies of systemic and tumor-infiltrating CD8+ and CD4 + T cells, increased proportion of PD-1 + T and NK cells, and increased PD-L1 expression by tumor cells. We propose that E2 reduces anticancer lymphoid cell infiltration into tumors and increases their exhaustion status, preventing Zol-induced activation of T and NK cells. Our data suggest that under premenopausal concentrations of E2, the anti-tumor response to Zol can be restored by blocking PD-1/PD-L1 interactions.

Methods

Cell lines

Cell lines used were triple-negative, bone-homed mouse mammary E0771 (kind gift from Prof Sandra McAllister (Harvard University, Boston, USA)) and 4T1 (purchased from the European Cell Culture Collection), stably transfected with luciferase (LUC-2). Cells were cultured in RPMI 1640 medium supplemented with glutaMAX™ (GIBCO) and 10% fetal bovine serum (FBS) (Sigma-Aldrich, UK).

Mouse models

All mice were purchased from Charles River Laboratories (Kent, UK) and mice maintained on a 12 h light: 12 h dark cycle with free access to food and water. All studies were carried out in accordance with local guidelines and under Home Office approval under project licenses P99922A2E and PP8941613, University of Sheffield, UK.

Mouse models representing pre- and postmenopausal E2 were generated through ovariectomising 12–14-week-old female C57BL/6 or BALB/c mice (Charles River, UK) and supplementing with 0 or 12.5 mg/L 17ß-estradiol (E2; Sigma Aldrich, Poole UK) via drinking water plus addition of 40ug/kg/day goserelin (goserelin acetate, Sigma Aldrich, UK), to prevent ovariectomy-induced changes in FSH. Metastasis was instigated by intracardiac injection of either 50,000 4T1-Luc2 cells (BALB/c) or 25,000 E0771-Luc2 (C57BL/6) cells. Primary tumor growth was established by intramammary injection of 50,000 4T1-Luc2 cells or E0771-Luc2 cells. To determine the effects of pre- and postmenopausal concentrations of E2 +/− Zol on tumor growth and immune cell regulation, mice received subcutaneous injection of 100 µg/kg/week Zol (supplied as a disodium salt by Novartis) or PBS control, starting 3-days after tumor cell injection (Fig. 1a). Mice were culled 15 or 19 days after ovariectomy and lungs, spleen and long bones stored in 90% FBS/10% DMSO at −80 °C until immune cell analysis (n = 10/group).

For NK 1.1+ and CD8 + T cell depletion experiments, postmenopausal concentrations of E2 were modeled in 12–14-week-old female C57BL/6 (Fig. 8a). 5-days later subcutaneous injections of 100 µg anti-mouse CD8A Alpha antibody (Clone 2.43 BE0061, Bio X Cell, USA), 100 µg anti-mouse NK1.1 antibody (clone PK136, BE0036 Bio X Cell, USA) or 100ul inVivoPure pH 7.0 dilution buffer (control) every three days. 25,000 E0771-Luc2 cells were administered by intracardiac injection 2-days after the first antibody injection, and mice were administered 100 µg/kg/week Zol or PBS control 3-days later. Mice were culled on day 18, and successful

antibody depletion was confirmed by flow cytometric analysis of immune cells in bone and spleen.

To determine the effects of combining anti-PD-L1 or anti-PD-1 treatment with Zol, pre- and postmenopausal concentrations of E2 were modeled in 12–14-week-old female BALB/c mice ($n = 9$-12/group), which received an intracardiac injection of 50,000 4T1-Luc-2 cells. Mice were treated with 30 mg/kg/2-days mouse anti-PD-L1 antibody (supplied as a mouse equivalent to avelumab by Merck KGaA, Germany) or 250 µg/mouse/3-days anti-mouse PD-1 antibody (clone RMP1-14, IVMB0037, Assay Genie Ltd., Ireland), 100 µg/kg/week Zol, PBS control, or combination treatments. Mice were culled 9 days after tumor cell injection, and lungs, spleen, and long bones were stored in 90% FBS/10% DMSO at −80 °C for downstream analysis (Fig. 9).

Measurement of tumor burden

Tumor growth was monitored in live mice using an IVIS Lumina II system (PerkinElmer, USA) or an IVIS Spectrum Imaging System (PerkinElmer, USA). Mice were imaged by dorsal and ventral exposure 5 min after subcutaneous injection of 30 mg/kg of D-Luciferin (Invitrogen, UK). Tumor location was confirmed postmortem following dissection of the hind limbs and soft tissues (lungs, liver, spleen, and kidneys). All images were analyzed by creating a region of interest (ROI) around the tumor(s); luminescence signal was acquired in radiance (photons/second) under the same threshold setting.

Flow cytometry

Frozen spleens, lung tissues, or bone marrow were rapidly thawed in a 37 °C water bath and washed three times with cold 10% (v/v) FBS in PBS to remove DMSO. Thawed spleen and lung tissues were dissociated and passed through a 70–100 µm cell strainer to generate single-cell suspensions in 10% (v/v) FBS/PBS.

Cells were aliquoted into control groups (unstained, single-stained, and fluorescence-minus-one [FMO] controls) and experimental samples. All samples were incubated with fluorochrome-conjugated antibodies (Supplementary Tables 1–2) and a viability dye for 45 min on ice, protected from light. Following incubation, cells were washed and resuspended in 400 µL of 4% (v/v) paraformaldehyde (PFA, Fisher Chemical, 1900271) in PBS. The cell suspension was then filtered into Falcon™ tubes (352235) and analyzed using either a BD LSR II or a Cytek Aurora 5 flow cytometer. Data were analyzed using software v10.8.0 or SpectroFlo v3.3.0. Single-cell staining control and gating strategies are shown in Supplementary Figs. 8–15. For lymphoid cells: T cells were identified as CD45+ CD3+ CD19−; CD4 + T cells identified as CD45+ CD3+ CD19− CD4+ CD8−; Treg cells identified as CD45+ CD3+ CD19− CD4+ CD8− CD25+ Foxp3+; CD8 + T cells identified as CD45+ CD3+ CD19− CD8+ CD4−; NK cells identified as CD45+ CD3− CD19− NK1.1+/CD49b+ and B cells identified as CD45+ CD3− CD19+. For myeloid cells: GMDSC cells were identified as CD45+ Ly6G+ CD11b+; monocytes identified as CD45+ Ly6G− CD11b+ $Ly6C^{high}$; macrophages identified as CD45+ Ly6G− CD11b+ $Ly6C^{low}$ F4/80+; M2- macrophage identified as CD45+ Ly6G− CD11b+ $Ly6C^{low}$ F4/80+ CD206+ ; dendritic cells identified as CD45+ Ly6G− Ly6C− MHCII+ CD11c+.

Cancer- immune cell co-cultures

NK cells and CD8 + T cells were isolated from mouse spleens using the Mouse NK 1.1 or CD8 + T Cell Isolation Kits according to the manufacturer's specifications (STEMCELL #19855 and #19853, respectively). 1×10^6/mL NK 1.1 or CD8+ cells were co-cultured with 5×10^4/mL 4T1 or E0771 cells in phenol red-free RPMI-1640 medium (11835-030, Gibco, USA) supplemented with 10% v/v FBS, 1% v/v P/S, 1% v/v 1 M HEPES (SH30237.01, Cytiva, UK), and 0.1% v/v 50 mM 2-Mercaptoethanol (31350-010, Gibco, USA) for 48 h. Tumor cell apoptosis/viability was measured by Annexin V/propidium iodide staining and flow cytometry as follows: Cells were collected and resuspended in the FACS buffer (10% v/v FBS in PBS) before being incubated with a BV421-conjugated CD45 antibody (1:100 working dilution; Biolegend, 103134) for 30 minutes on ice, followed by washing with PBS. The cells were then resuspended in 50 µL 1X Annexin binding buffer (422201, Biolegend, UK) and incubated with APC-conjugated Annexin V (640920, Biolegend, UK) and 5 µL of 1 mg/ml propidium iodide (PI) solution (P4170, Sigma-Aldrich, USA), according to the manufacturer's instructions. Flow cytometry was performed using a Cytek Aurora 5 flow cytometer. Data were manually gated using SpectroFlo software v3.3.0 to exclude doublets, debris, and $CD45^+$ leukocytes.

Biochemical analysis

Serum concentrations of estradiol were assessed using a Mouse/Rat Estradiol ELISA kit (ES180S-100 CALBIOTECH, USA) in accordance with the manufacturer's instructions.

Western blotting

Primary 4T1/E0771 tumors were isolated from the mammary fat pads of ovariectomized BALB/c / C57BL/6 mice supplemented with 0 or 12.5 mg/L 17ß-estradiol 2-weeks after injection. Tumors were snap-frozen following dissection and stored at −80 °C prior to protein extraction using the mammalian cell lysis kit (MCL-1: Sigma-Aldrich). Fifteen micrograms of total protein were separated on a Bio-rad precast 4%–15% gel, then transferred onto a PVDF membrane (Pierce, ThermoFisher, Loughborough, UK). Non-specific binding was blocked in 1X casein solution (B6429, Sigma Aldrich) before incubating with rabbit anti-mouse PD-L1 (EPR20529, Abcam, Cambridge, UK)/rat anti-mouse PD-L1 (14-5982-82, Invitrogen, California, USA) at a concentration of 1:500 or rabbit- anti mouse GAPDH (EPR16884, Abcam)/HRP-conjugated GAPDH Monoclonal antibody (HRP-60004, Proteintech, Rosemont, USA) in 1X casein overnight at 4 °C. Secondary antibody was rabbit HRP (P0448; Dako, Glostrup, Denmark) at 1/5000 for 1 h at room temperature. HRP was detected using the West Femto Chemiluminescent Detection Kit (Pierce, ThemoFisher) on the BioRad ChemiDoc MP (Bio-Rad, Watford, UK).

Analysis of patient samples

All human samples were obtained following written, informed consent from patients, and studies were conducted in accordance with the Declaration of Helsinki. PD-L1 expression was assessed following immunohistochemical staining using the FDA approved PD-L1 (28-8) antibody on tissue microarrays (TMAs) containing 3-separate primary tumor cores/patient taken from 1729 patients included in the clinical trial AZURE. (Sponsored by the University of Sheffield and approved as a United Kingdom national trial by the Clinical Trials Committee; controlled trials ethical approval number ISRCTN79831382 [14]). These samples were obtained from patients with grade II and III breast cancer, without evidence of metastasis. Patients were subsequently randomized to standard adjuvant therapy with or without addition of Zol for 5-years and followed up for 10-years [14]. TMAs contained 3-separate cores per patient, were stained for PD-L1, and scored blindly for the presence or absence of PD-L1. Tumor cell PD-L1 expression was then linked with biochemically confirmed menopausal status, overall survival, disease recurrence at any site, or disease recurrence specifically in bone.

Statistics

For experiments using animal models and non-clinical material, groupwise comparisons were performed using the ANOVA test followed by Tukey's post-hoc test or unpaired student t test using the GraphPad Prism 10 software, as indicated on individual figures. P values are presented as * < 0.05, ** < 0.01, *** < 0.001, **** < 0.0001. For analysis of clinical samples, clinical samples, a Cox proportional hazards model, using the R statistical software (v. 4.4.1), was used to investigate the effect of PD-L1 expression on overall survival, disease-free survival, recurrence in any site, and recurrence in bone in the presence or absence of Zol. Statistical significance was determined using two-sided P values < 0.05.

Data availability

The datasets generated and analyzed during the current study are not publicly available, as no suitable publicly accessible databases exist to deposit this type of data. Data and/or material from mouse models are available from the corresponding author on reasonable request.

Received: 15 April 2026; Accepted: 31 August 2026;
Published online: 23 October 2026

References

1. Coleman, R. et al. Adjuvant zoledronic acid in patients with early breast cancer: final efficacy analysis of the AZURE (BIG 01/04) randomised open-label phase 3 trial. *Lancet Oncol.* **15**, 997–1006 https://doi.org/10.1016/S1470-2045(14)70302-X (2014).
2. UK, B. C. *Facts and Figures Breast Cancer UK* (2022).
3. Yuan, J., Xin, F. & Wang, R. ANXA2 regulates RANKL-induced osteoclast differentiation through STAT3 signaling in breast cancer. *Breast Cancer* **17**, 837–849 https://doi.org/10.2147/BCTT.S542181 (2025).
4. Zambelli, A. et al. The use of bone-modifying agents in early breast cancer: AIOM Guidelines update and perspectives. *Tumori*, https://doi.org/10.1177/03008916251367339, 3008916251367339 (2025).
5. Russell, R. G. Bisphosphonates: the first 40 years. *Bone* **49**, 2–19 https://doi.org/10.1016/j.bone.2011.04.022 (2011).
6. Van Acker, H. H., Anguille, S., Willemen, Y., Smits, E. L. & Van Tendeloo, V. F. Bisphosphonates for cancer treatment: mechanisms of action and lessons from clinical trials. *Pharm. Ther.* **158**, 24–40 https://doi.org/10.1016/j.pharmthera.2015.11.008 (2016).
7. Hiraga, T., Williams, P. J., Ueda, A., Tamura, D. & Yoneda, T. Zoledronic acid inhibits visceral metastases in the 4T1/luc mouse breast cancer model. *Clin. Cancer Res.* **10**, 4559–4567 https://doi.org/10.1158/1078-0432.CCR-03-0325 (2004).
8. Neville-Webbe, H. L., Evans, C. A., Coleman, R. E. & Holen, I. Mechanisms of the synergistic interaction between the bisphosphonate zoledronic acid and the chemotherapy agent paclitaxel in breast cancer cells in vitro. *Tumour Biol.* **27**, 92–103 https://doi.org/10.1159/000092489 (2006).
9. Ottewell, P. D. et al. Differential effect of doxorubicin and zoledronic acid on intraosseous versus extraosseous breast tumor growth in vivo. *Clin. Cancer Res.* **14**, 4658–4666 https://doi.org/10.1158/1078-0432.CCR-07-1545 (2008).
10. Ottewell, P. D. et al. Antitumor effects of doxorubicin followed by zoledronic acid in a mouse model of breast cancer. *J. Natl. Cancer Inst.* **100**, 1167–1178 https://doi.org/10.1093/jnci/djn240 (2008).
11. Ottewell, P. D. et al. Anticancer mechanisms of doxorubicin and zoledronic acid in breast cancer tumor growth in bone. *Mol. Cancer Ther.* **8**, 2821–2832 https://doi.org/10.1158/1535-7163.MCT-09-0462 (2009).
12. Gnant, M. et al. Adjuvant endocrine therapy plus zoledronic acid in premenopausal women with early-stage breast cancer: 62-month follow-up from the ABCSG-12 randomised trial. *Lancet Oncol.* **12**, 631–641 https://doi.org/10.1016/S1470-2045(11)70122-X (2011).
13. Coleman, R. et al. Zoledronic acid (zoledronate) for postmenopausal women with early breast cancer receiving adjuvant letrozole (ZO-FAST study): final 60-month results. *Ann. Oncol.* **24**, 398–405 https://doi.org/10.1093/annonc/mds277 (2013).
14. Kolberg, H. C. et al. Breast cancer 2012 - New aspects. *Geburtshilfe Frauenheilkd.* **72**, 602–615 https://doi.org/10.1055/s-0032-1315131 (2012).
15. Mobus, V. et al. German adjuvant intergroup node-positive study (GAIN): a phase III trial comparing two dose-dense regimens (iddEPC versus ddEC-PwX) in high-risk early breast cancer patients. *Ann. Oncol.* **28**, 1803–1810 https://doi.org/10.1093/annonc/mdx203 (2017).
16. Wilson, C., Ottewell, P., Coleman, R. E. & Holen, I. The differential anti-tumour effects of zoledronic acid in breast cancer - evidence for a role of the activin signaling pathway. *BMC Cancer* **15**, 55 https://doi.org/10.1186/s12885-015-1066-7 (2015).
17. Canuas-Landero, V. G. et al. Oestradiol contributes to differential antitumour effects of adjuvant zoledronic acid observed between pre- and post-menopausal women. *Front. Endocrinol.* **12**, 749428 https://doi.org/10.3389/fendo.2021.749428 (2021).
18. Weber, M. et al. Zoledronate causes a systemic shift of macrophage polarization towards M1 in vivo. *Int. J. Mol. Sci*. **22**, https://doi.org/10.3390/ijms22031323 (2021).
19. Sugie, T. et al. Zoledronic acid-induced expansion of gammadelta T cells from early-stage breast cancer patients: effect of IL-18 on helper NK cells. *Cancer Immunol. Immunother.* **62**, 677–687 https://doi.org/10.1007/s00262-012-1368-4 (2013).
20. Liu, H. et al. Immune modulation of CD4(+)CD25(+) regulatory T cells by zoledronic acid. *BMC Immunol.* **17**, 45 https://doi.org/10.1186/s12865-016-0183-7 (2016).
21. George, C. N. et al. Oestrogen and zoledronic acid driven changes to the bone and immune environments: potential mechanisms underlying the differential anti-tumour effects of zoledronic acid in pre- and post-menopausal conditions. *J. Bone Oncol.* **25**, 100317 https://doi.org/10.1016/j.jbo.2020.100317 (2020).
22. Ottewell, P. D. et al. Sustained inhibition of tumor growth and prolonged survival following sequential administration of doxorubicin and zoledronic acid in a breast cancer model. *Int. J. Cancer* **126**, 522–532 https://doi.org/10.1002/ijc.24756 (2010).
23. Eisen, A. et al. Use of adjuvant bisphosphonates and other bone-modifying agents in breast cancer: ASCO-OH (CCO) guideline update. *J. Clin. Oncol.* **40**, 787–800 https://doi.org/10.1200/JCO.21.02647 (2022).
24. Coleman, R. et al. Bone health in cancer: ESMO clinical practice guidelines. *Ann. Oncol.* **31**, 1650–1663 https://doi.org/10.1016/j.annonc.2020.07.019 (2020).
25. Zagami, P. & Carey, L. A. Triple negative breast cancer: pitfalls and progress. *NPJ Breast Cancer* **8**, 95 https://doi.org/10.1038/s41523-022-00468-0 (2022).
26. Zhang, Y. et al. Estrogen protects against renal ischemia-reperfusion injury by regulating Th17/Treg cell immune balance. *Dis. Markers* **2022**, 7812099 https://doi.org/10.1155/2022/7812099 (2022).
27. Hartmann, W., Blankenhaus, B., Brunn, M. L., Meiners, J. & Breloer, M. Elucidating different pattern of immunoregulation in BALB/c and C57BL/6 mice and their F1 progeny. *Sci. Rep.* **11**, 1536 https://doi.org/10.1038/s41598-020-79477-7 (2021).
28. Lehmann, B. D. et al. Multi-omics analysis identifies therapeutic vulnerabilities in triple-negative breast cancer subtypes. *Nat. Commun.* **12**, 6276 https://doi.org/10.1038/s41467-021-26502-6 (2021).
29. Carlyle, J. R. et al. Molecular and genetic basis for strain-dependent NK1.1 alloreactivity of mouse NK cells. *J. Immunol.* **176**, 7511–7524 https://doi.org/10.4049/jimmunol.176.12.7511 (2006).
30. Hansda, A. K., Biswas, B. & Goswami, R. 17-beta Estradiol (E2) distinctly regulates the expression of IL-4 and IL-13 in Th2 cells via modulating the interplay between GATA3 and PU.1. *Cytokine* **173**, 156440 https://doi.org/10.1016/j.cyto.2023.156440 (2024).
31. Yang, Y. et al. Abeta-damaged neural stem cells migration and differentiation through Wnt3a/beta-catenin pathway: Protective effects of 17beta-E2. *Neurosci. Lett.* **865**, 138350 https://doi.org/10.1016/j.neulet.2025.138350 (2025).
32. Byemerwa, J., Chang, C. Y. & McDonnell, D. P. The roles of natural killer cells in breast cancer pathobiology and their regulation by estrogens. *Endocr. Rev.* **46**, 690–708 https://doi.org/10.1210/endrev/bnaf014 (2025).
33. Chang, P. et al. Effect of estradiol valerate on humoral immune function in BALB/c mice after total hysterectomy. *Braz. J. Med. Biol.*

Res. **58**, e14651 https://doi.org/10.1590/1414-431X2025e14651 (2025).
34. Saito, T. et al. Estrogen contributes to gender differences in mouse ventricular repolarization. *Circ. Res.* **105**, 343–352 https://doi.org/10.1161/CIRCRESAHA.108.190041 (2009).
35. Song, S., Tang, H., Quan, W., Shang, A. & Ling, C. Estradiol initiates the immune escape of non-small cell lung cancer cells via ERbeta/SIRT1/FOXO3a/PD-L1 axis. *Int. Immunopharmacol.* **107**, 108629 https://doi.org/10.1016/j.intimp.2022.108629 (2022).
36. Yang, L. et al. Posttranscriptional control of PD-L1 expression by 17beta-Estradiol via PI3K/Akt signaling pathway in ERalpha-positive cancer cell lines. *Int. J. Gynecol. Cancer* **27**, 196–205 https://doi.org/10.1097/IGC.0000000000000875 (2017).
37. Li, H., Gu, W., Jeffery, P. & Chen, C. 17-beta-estradiol reduces surface PD-L1 expression in estrogen receptor-positive breast cancer but not type 1 endometrial cancer cells. *Clin. Transl. Med.* **13**, e1330 https://doi.org/10.1002/ctm2.1330 (2023).
38. George, J. et al. Genomic amplification of CD274 (PD-L1) in small-cell lung cancer. *Clin. Cancer Res.* **23**, 1220–1226 https://doi.org/10.1158/1078-0432.CCR-16-1069 (2017).
39. Ali, H. R. et al. PD-L1 protein expression in breast cancer is rare, enriched in basal-like tumours and associated with infiltrating lymphocytes. *Ann. Oncol.* **26**, 1488–1493 https://doi.org/10.1093/annonc/mdv192 (2015).
40. Dong, W., Li, J. & Zhuang, Z. Neutrophil-related signature characterizes immune landscape and predicts prognosis of invasive breast cancer. *Biochem. Genet.* **63**, 4464–4490 https://doi.org/10.1007/s10528-024-10940-0 (2025).
41. Gu, Y., Feng, Z., Xu, X. & Jin, L. Identification of a novel immune-related gene signature by single-cell and bulk sequencing for the prediction of the immune landscape and prognosis of breast cancer. *Cancer Cell Int.* **24**, 393 https://doi.org/10.1186/s12935-024-03589-7 (2024).
42. Yin, S. et al. A novel tumor-associated neutrophil-related risk signature based on single-cell and bulk RNA-sequencing analyses predicts the prognosis and immune landscape of breast cancer. *J. Cancer* **15**, 5655–5671 https://doi.org/10.7150/jca.100338 (2024).
43. Clezardin, P. et al. Bone metastasis: mechanisms, therapies, and biomarkers. *Physiol. Rev.* **101**, 797–855 https://doi.org/10.1152/physrev.00012.2019 (2021).
44. Ottewell, P. D. et al. Zoledronic acid has differential antitumor activity in the pre- and postmenopausal bone microenvironment in vivo. *Clin. Cancer Res.* **20**, 2922–2932 https://doi.org/10.1158/1078-0432.CCR-13-1246 (2014).
45. Mundy, G. R. Bisphosphonates as cancer drugs. *Hosp. Pract.* **34**, 81-84, 88-89, 93-84 https://doi.org/10.3810/hp.1999.05.141 (1999).
46. Moretti, L. et al. Adjuvant denosumab for early breast cancer-evidence and controversy. *Breast* **78**, 103826 https://doi.org/10.1016/j.breast.2024.103826 (2024).
47. Coleman, R. et al. Adjuvant denosumab in early breast cancer (D-CARE): an international, multicentre, randomised, controlled, phase 3 trial. *Lancet Oncol.* **21**, 60–72 https://doi.org/10.1016/S1470-2045(19)30687-4 (2020).
48. Chen, H., Xu, Z. & Varner, J. Targeting myeloid cells to improve cancer immune therapy. *Front. Immunol.* **16**, 1623436 https://doi.org/10.3389/fimmu.2025.1623436 (2025).
49. Obeagu, E. I. N1 and N2 neutrophil subtypes in breast cancer: functional implications and clinical perspectives: a narrative review. *Ann. Med. Surg.* **87**, 5762–5769 https://doi.org/10.1097/MS9.0000000000003609 (2025).

Acknowledgements

The authors would like to thank all patients who took part in the AZURE trial as well as Weston Park Cancer Charity and Yorkshire Cancer Research for funding this work on research grants: CA175 and YCRSPF/2023/137, respectively. We would also like to thank the flow cytometry core facility staff, especially Mrs Susan Gauntlet and Dr Mark Jones, for their input in multicolor flow cytometry panel designs. Mr Matthew Fisher for his expert input into the in vivo experiments and Mrs Orla Gallagher for tissue processing.

Author contributions

Concept and funding acquisition P.D.O., I.H., M.M., M.W., S.D., C.W. and F.T.; Data acquisition, analysis, and interpretation C.G., J.Z., V.C., P.D.O., D.V.L., R.H., L.Q. and M.J.; Statistical analysis M.D.; Provision of tissue samples J.B., Writing and editing the manuscript P.D.O., J.Z., I.H., M.M., M.W., J.E., C.G., S.D., T.H., L.Q., R.H., C.W.

Competing interests

The authors declare no competing interests.

Additional information

Supplementary information The online version contains supplementary material available at https://doi.org/10.1038/s41523-026-01048-2.

Correspondence and requests for materials should be addressed to Penelope D. Ottewell.

Reprints and permissions information is available at http://www.nature.com/reprints

Publisher's note Springer Nature remains neutral with regard to jurisdictional claims in published maps and institutional affiliations.

Open Access This article is licensed under a Creative Commons Attribution 4.0 International License, which permits use, sharing, adaptation, distribution and reproduction in any medium or format, as long as you give appropriate credit to the original author(s) and the source, provide a link to the Creative Commons licence, and indicate if changes were made. The images or other third party material in this article are included in the article's Creative Commons licence, unless indicated otherwise in a credit line to the material. If material is not included in the article's Creative Commons licence and your intended use is not permitted by statutory regulation or exceeds the permitted use, you will need to obtain permission directly from the copyright holder. To view a copy of this licence, visit http://creativecommons.org/licenses/by/4.0/.

© The Author(s) 2026

This Article in Press is shared early to give you faster access to new research. It is citable and carries a permanent DOI. The final edited version will replace it automatically.